TEMPERATURE AND DENSITY STRUCTURE OF HOT AND COOL LOOPS DERIVED FROM THE ANALYSIS OF TRACE DATA

P. Testa[1], G. Peres[1], F. Reale[1], and S. Orlando[2]

[1]Dip. Scienze Fisiche e Astronomiche, Università di Palermo, Piazza del Parlamento,1, I-90134, Palermo, Italy
[2]Osservatorio Astronomico G.S.Vaiana, Piazza del Parlamento,1, I-90134, Palermo, Italy

ABSTRACT

We address the plasma structuring both *across* and *along* the magnetic field in two sets of solar coronal loops, observed with TRACE in the 171Å and 195Å passbands. We derive, after proper background removal, the density stratification and the thermal structure of the plasma in the fibrils forming the loops with two techniques: a) filter ratio diagnostic (195Å/171Å) and b) modeling intensity profiles along the fibrils with hydrostatic models.

We find evidence of a hot fibril ($T \sim 5 \cdot 10^6$ K), with temperature and density stratification well-described with a typical non-isothermal hydrostatic loop model, and evidence of rather cold fibrils ($T \sim 2 \cdot 10^5$ K), isothermal and probably in dynamic conditions.

Key words: Loops filamentation; hydrostatic models; TRACE.

1. INTRODUCTION

We aim at studying the internal structure of coronal loops in terms of the properties of single fibrils, i.e. with a different approach with respect to previous analysis of coronal loops observed with TRACE (e.g. Lenz et al. 1999; Aschwanden et al. 2000) which studied bundles of fibrils as single coronal loops.

The upper panel of Fig. 1 shows that TRACE 195Å/171Å filter ratio is a multi-valued function of temperature. The *standard analysis* of TRACE data selects a temperature range, $0.9 \div 1.8 \cdot 10^6$ K, where R(T) is invertible and excludes any other temperature range. However, this assumption does not take into account the influence of the emission measure on the plasma visibility. For example, for Rosner, Tucker & Vaiana (1978) or Serio et al. (1981; hereafter S81) hydrostatic loop models, we find that, for fixed loops length, approximately $n \propto T^2$ and then $EM \propto n^2 \propto T^4$, so the visibility with TRACE of the coronal confined plasma keeps high also at temperature of several MK, as shown in Fig. 1. These considerations have stimulated us to follow a new multi-way approach that provides us with cross-checks and allows us to build a robust and consistent scenario.

2. TRACE DATA

We have selected structures on the disk where the background had a simple structure and therefore it was easier

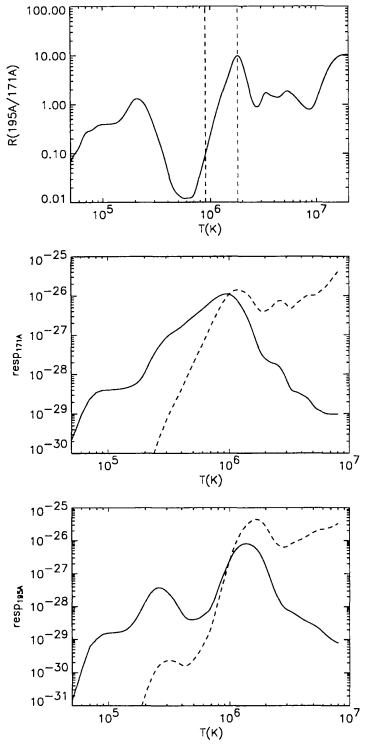

Figure 1: Upper panel – Filter ratio (195Å/171Å) vs. temperature; the dashed lines delimit the range considered by the *standard analysis* for the temperature derivation. Central and lower panel – solid lines: TRACE response curves in the two bands, 171Å (center) and 195Å (lower) (Bentley 2000); dashed lines: TRACE sensitivity in the two narrow bands to the emission of plasma in hydrostatic loops with fixed length, considering the scaling law of Rosner, Tucker&Vaiana (1978).

Proc. 'SOLMAG: Magnetic Coupling of the Solar Atmosphere Euroconference and IAU Colloquium 188' Santorini, Greece, 11-15 June 2002 (ESA SP-505, October 2002)

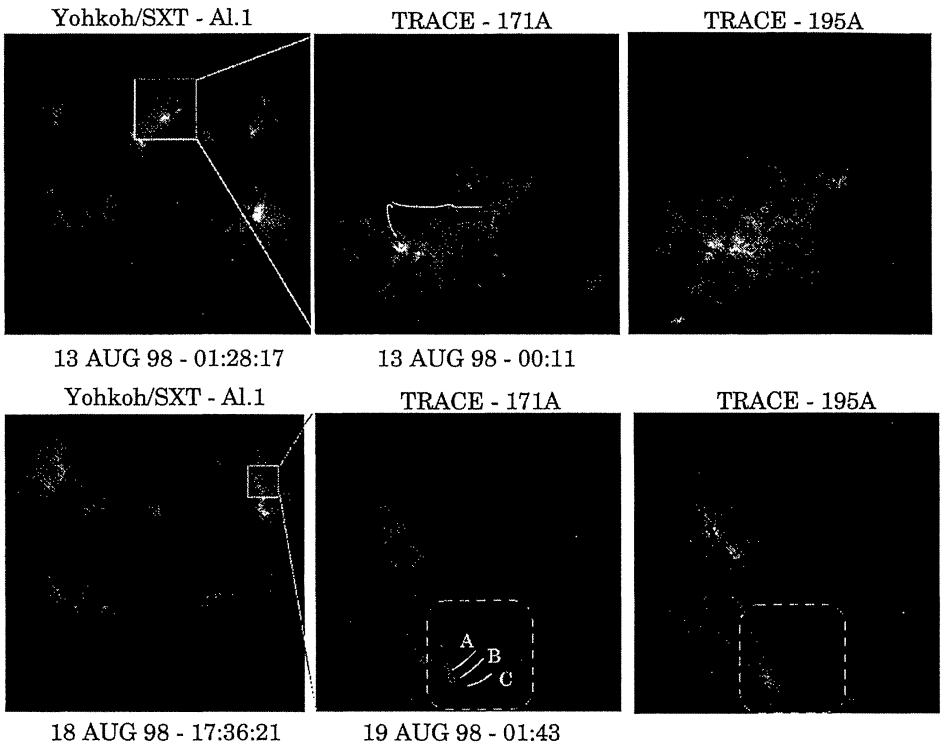

Figure 2: Images of the coronal structures analyzed, all belonging to the same AR but observed six days apart. Upper panels – left: full disk Yohkoh/SXT image through the filter Al.1, together with the field of view of TRACE; center and right: TRACE images in the two bands, 171Å and 195Å; the white line marks the fibril analyzed in detail. Lower panels – As in the upper panels, for the data collected six days later; the dashed box contains the fibrils analyzed, marked with the white lines.

to isolate the emission of the structure of interest from that of coaligned ones. We selected two observations of the same active region (NOAA Active Region 8297) made, six days apart, with TRACE in August 1998 in two filter bands, 171Å and 195Å. Fig. 2 shows the TRACE observations and the relevant full-disk Yohkoh/SXT X-ray images.

3. METHOD OF ANALYSIS

We have derived T and EM profiles in the loop fibrils both through filter ratio diagnostic (I_{195}/I_{171}) in each pixel, and through comparison with hydrostatic loop models. At variance with the *standard analysis*, we consider the range of temperature where the filter response is larger than 0.1% of the peak, i.e. 10^5 K $< T < 10^7$ K; if a filter ratio matches more than one temperature value, we selected the temperature consistent with the best-fitting hydrostatic model.

3.1. Loop transversal structure

We analyzed the intensity profiles *across* loops sampling them along a few transversal paths, with care to avoid points of intersection with other bright coronal structures. To increase the signal to noise ratio we sum the signal over small strips, each 1 pixel wide and 8 pixels long, aligned with the fibrils. The background emission at each place along the loop is obtained as a rectilinear, lower envelope of the profile, through the interpolation between the profile minima. The thickness of the fibrils is defined operatively from the *transversal* intensity profiles as the width of the gaussian fitting the shape of the fibrils.

3.2. Loop longitudinal structure

We derived the intensity profiles *along* the fibrils over a path as close as possible to the fibril centre. The background emission is obtained taking, from each transversal background profile, the value at the fibril position, and then interpolating among them. Then we fitted, simultaneously in the two bands, the *longitudinal* intensity profiles with profiles synthesized from hydrostatic loop models: either an isothermal model, or a non-isothermal (S81) model that takes into account the detailed energy balance of the plasma inside the loop. We include, for both models, the effect of loop inclination (effective gravity component) deduced from morphological analysis. For the complete loop observed on August 13 we deduced an inclination of about 30°, i.e. approximately equal to the latitude, since it appears perpendicular to the line of sight. Whereas, the fibrils observed on August 19 are assumed perpendicular to the surface as they appear in the images.

For the isothermal model we fitted the background subtracted profiles along one loop leg with:

$$I_f(s) = A_f \cdot e^{-(s-s_0)/L}$$

where L is the brightness scale-height, which depends just on temperature, s_0 is a reference point and A_f is a normalization factor depending on the squared density, the column depth, the exposure time and the filter response. For the complete loop observed on August 13, we use an exponential for each leg, and s_0 is the pixel where the profiles of the two legs match at the loop apex. The fitting parameters of this model are: the scale-length of the exponential (i.e. the isothermal temperature), the normalisation constants in each bands and s_0.

As for the S81 loop model, taking the loop length from the images, we generated a set of 100 models with maximum temperature in the range 10^5 K $\div 10^7$ K, equally spaced in maximum temperature T_{max} with constant $\Delta log T_{max} = 0.02$; the base pressure is tied to the temperature by the scaling laws. The fitting function in this case is:

$$I_f(s) = \alpha_f \cdot n^2(s) \cdot R_f(T(s))$$

where α_f is a normalisation constant proportional to the emitting plasma volume and $R_f(T)$ is the filter response vs. temperature got from the CHIANTI (Dere et al., 1997) model and folding with the instrument spectral response. The parameters of the fit for this model are: the loop maximum temperature, T_{max}, the two normalization constants and the symmetry center of the model relative to the observed profiles. The best fit model is that yielding the lowest χ^2 value in the parameter space.

4. RESULTS

4.1. August 13 data

A system of extended coronal loops with length of about 10^{10}cm is well visible (Fig. 2). As for the filamentation transversal to the magnetic field, we found that both the thickness of the fibrils and the distance between them appear to increase from the footpoint to the apex. We found for the fibrils widths in a wide range: $1.8 \cdot 10^8 \div 10^9$ cm. The analysis of the transversal structure yielded values of 195Å/171Å fluxes ratios, inside the fibrils, approximately in the range $1 \div 2$, corresponding to temperature of $\sim 1.5 \cdot 10^6$ K or, rather of a few million degrees (see Fig. 1). Through the analysis of the emission characteristics along the loop we have been able to discriminate between the different temperature ranges and to derive a temperature.

The fibril marked in Fig. 2, because of its complete visibility, allowed us to constrain the fitting of the longitudinal structure. To increase the signal to noise ratio, we binned the longitudinal emission profiles over 4 pixels (its half length is about 250 pixels, corresponding to $\approx 9 \cdot 10^9$ cm); we excluded the noisy region close to the footpoints. The isothermal loop model best fitting the 171Å and 195Å observed profiles is at $T = 2.2 \cdot 10^6$ K but the reduced χ^2 is $\chi^2_r = 2.1$. Instead the best-fitting S81 model shows a much better agreement with the data as shown in Table 1. Fig. 3 shows the data and the best fit model: the agreement is clearly good (and, in fact, $\chi^2_r \approx 1.1$). The temperature, $\sim 5 \cdot 10^6$ K, is compatible with the filter ratio found at various points with the analysis of transversal structure. We found a second local χ^2 minimum, at $T_{max} \sim 7 \cdot 10^5$ K, excluded because of much higher χ^2 value ($\chi^2_r \sim 2$), because this temperature is not compatible with the fluxes ratios observed, and because the normalization constants, very different in the two bands, lead to column depths values ranging between 10^{12}cm and 10^{13}cm.

Table 1: Best-fit parameters of non-isothermal model .

Length of the loop	$8.8 \cdot 10^9$ cm
Temperature at loop apex	$5.2 \pm 0.3 \cdot 10^6$ K
Pressure at the base	5.2 ± 0.8 dyn/cm^2
Density at loop apex	$3.2 \pm 0.3 \cdot 10^9$ cm^{-3}
Column depth in 171Å band	$3.8 \pm 0.5 \cdot 10^9$ cm
Column depth in 195Å band	$2.5 \pm 0.4 \cdot 10^9$ cm
χ^2_r	1.1
degrees of freedom	196

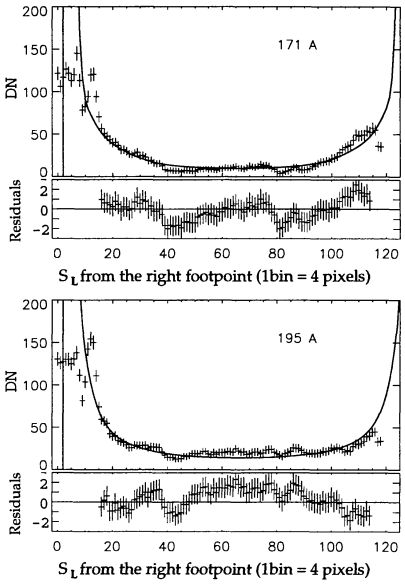

Figure 3: *Longitudinal* intensity profiles at 171Å and 195Å for the semicircular fibril observed on August 13, 1998. data points: rebinned measured values (1 bin = 4 pixels); solid lines: intensity profiles synthesized from the parameters of the best fitting S81 hydrostatic loop model. Below each graph we show the related fit residuals.

4.2. August 19 data

The fibrils observed on August 19 close to the limb appear very similar to each other as for both luminosity and morphology. These fibrils, observed over several hours, showed some slow variability in brightness, while, neither their geometry nor their length appeared to vary. Studying their transversal structure we found that they have similar thickness, almost constant along the fibrils, in a range $1.4 \div 4.2 \cdot 10^8$ cm ($2 \div 6$ pixels); the lower values are comparable to the spatial resolution of TRACE.

Table 2: Best-fit parameters of isothermal model.

fibril	T (10^5 K)	n_{base} (10^{10} cm^{-3})		χ^2_r	dof
		171Å	195Å		
A	$2.7^{+1.2}_{-0.6}$	$0.7^{+0.5}_{-0.3}$	$0.9^{+0.8}_{-0.1}$	0.24	48
B	$1.8^{+0.2}_{-0.2}$	$3.4^{+0.7}_{-0.8}$	$3.5^{+1.9}_{-1.1}$	0.27	60
C	$2.6^{+1.2}_{-0.7}$	$0.5^{+0.5}_{-0.2}$	$1.0^{+1.0}_{-0.1}$	0.14	65

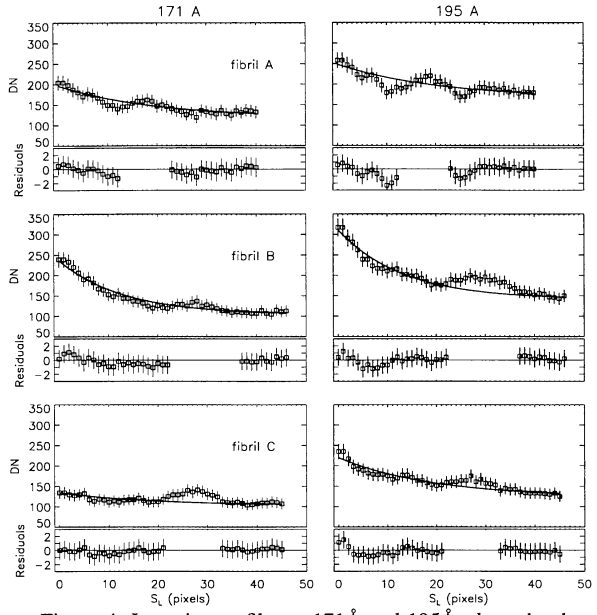

Figure 4: Intensity profiles at 171Å and 195Å *along* the three fibrils observed on August 19, 1998 (data points). The solid lines are synthesized from the temperature and density profile of the best fitting *isothermal* loop model.

As for the structure *along* the fibrils, in this case we could not constrain a complex loop model having only a small fraction of the loop; on the other hand, we found no evidence of thermal stratification along the fibrils. In fact the exponential trend of the isothermal model adequately describes the profiles along the three fibrils. Fig. 4 shows the best-fit model profiles superimposed to the data. In both 171Å and 195Å profiles, and for all the three fibrils considered, we excluded from the fitting the evident bump, due to another bright structure running across the fibrils. The parameters of the best-fit model for these three fibrils are in Table 2. The models best fitting all the three fibrils have a temperature of $\sim 2 \cdot 10^5$K, consistent with the filter ratio values from the transversal structure analysis. The analysis in both bands yields density values of the order of 10^{10} cm^{-3} in good agreement from the two bands.

5. DISCUSSION AND CONCLUSIONS

The fibrils observed on August 13 have a rather different width, in the range $4 \cdot 10^8 - 2 \cdot 10^9$ cm, and the width of each fibril appears to vary with height, in some case up to a factor 2. Instead, the selected fibrils of August 19 look more similar to each other with characteristic width of $\sim 3 \cdot 10^8$ cm, close to the spatial resolution limit, and their width is constant with height.

The two fibrils systems studied also show very different physical characteristics. The entirely visible fibril of August 13 shows a fairly good agreement with a S81 hydrostatic loop model at a rather high maximum temperature (~5 MK); an isothermal model cannot instead reproduce the observed profiles. Notice that with both models we invariably find a best fit temperature rather higher than 1 MK. The presence of such a hot loop is consistent with the almost simultaneous Yohkoh/SXT observations of the same region (Testa et al. 2002). At variance with the results of Aschwanden et al.(2000) and Lenz et al.(1999), our work shows the presence in TRACE data of a variety of loops over a large range of temperature, some isothermal and others not compatible with an isothermal plasma; also there is probably a class of structures at several million degrees typical of Yohkoh observations but also visible with TRACE.

As for the fibrils observed in August 19 an isothermal model with a temperature of $\sim 2 \cdot 10^5$K and a density n $\sim 10^{10}$cm^{-3} well describe all the three fibrils considered. We found that our findings for these cold loops are consistent with the simultaneous UV TRACE observations at 1550Å and 1600Å, more sensitive to colder plasma (Testa et al. 2002).

In the light of the above discussion, we found temperature and density distributions typical of hot coronal loops for the fibrils observed in August 13, near the central meridian, whereas the fibrils observed near the limb on August 19 is characterized by a much lower temperature and the absence of any evident thermal structuring. Notice that in both cases studied in detail we found a rather different scenario with respect to that of loops at $T \sim 10^6$ K, invariably found with *standard analysis*, and probably more complex than discussed by Aschwanden et al. (2000).

REFERENCES

Aschwanden, M.J., Nightingale, R.W., & Alexander, D. 2000, ApJ, 541, 1059

Bentley, R.D. 2000, SolarSoft TRACE Analysis Guide, MSSL UCL

Dere, K.P., Landi, E., Mason, H.E., Monsignori Fossi, B.C., & Young, P.R. 1997, AAS, 125, 149

Handy, B.N. et al. 1999, Solar Phys., 187, 229

Lenz, D.D., DeLuca, E.E., Golub, L., Rosner, R., & Bookbinder, J.A. 1999, ApJ, 517, L155

Rosner, R., Tucker, W.H., & Vaiana, G.S. 1978, ApJ, 220, 643

Serio, S., Peres, G., Vaiana, G.S., Golub, L., & Rosner, R. 1981, ApJ, 243, 288

Testa, P., Peres, G., Reale, F., Orlando, S. 2002, ApJ submitted

Tsuneta, S. et al. 1991, Solar Phys., 136, 37